

## Tuning the transport gap of functionalized graphene via electron beam irradiation

This content has been downloaded from IOPscience. Please scroll down to see the full text.

2013 New J. Phys. 15 033024

(<http://iopscience.iop.org/1367-2630/15/3/033024>)

View [the table of contents for this issue](#), or go to the [journal homepage](#) for more

### Download details:

IP Address: 144.173.57.81

This content was downloaded on 25/04/2016 at 11:30

Please note that [terms and conditions apply](#).

## Tuning the transport gap of functionalized graphene via electron beam irradiation

Steven E Martins<sup>1</sup>, Freddie Withers<sup>1</sup>, Marc Dubois<sup>2</sup>,  
Monica F Craciun<sup>1</sup> and Saverio Russo<sup>1,3</sup>

<sup>1</sup> Centre for Graphene Science, CEMPS, University of Exeter, Exeter EX4 4QL, UK

<sup>2</sup> Clermont Université, UBP, Laboratoire des Matériaux Inorganiques, CNRS-UMR 6002, F-63177 Aubière, France

E-mail: [S.Russo@exeter.ac.uk](mailto:S.Russo@exeter.ac.uk)

*New Journal of Physics* **15** (2013) 033024 (10pp)


Received 26 September 2012

Published 20 March 2013

Online at <http://www.njp.org/>

doi:10.1088/1367-2630/15/3/033024

**Abstract.** We demonstrate a novel method to tune the energy gap  $\epsilon_1$  between the localized states and the mobility edge of the valence band in chemically functionalized graphene by changing the coverage of fluorine adatoms via electron-beam irradiation. From the temperature dependence of the electrical transport properties we show that  $\epsilon_1$  in partially fluorinated graphene  $\text{CF}_{0.28}$  decreases upon electron irradiation up to a dose of  $0.08 \text{ C cm}^{-2}$ . For low irradiation doses ( $< 0.1 \text{ C cm}^{-2}$ ) partially fluorinated graphene behaves as a lightly doped semiconductor with impurity bands close to the conduction and valence band edges, whereas for high irradiation doses ( $> 0.2 \text{ C cm}^{-2}$ ) the electrical conduction takes place via Mott variable range hopping.

 Online supplementary data available from [stacks.iop.org/NJP/15/033024/mmedia](http://stacks.iop.org/NJP/15/033024/mmedia)

<sup>3</sup> Author to whom any correspondence should be addressed.



Content from this work may be used under the terms of the [Creative Commons Attribution-NonCommercial-ShareAlike 3.0 licence](http://creativecommons.org/licenses/by-nc-sa/3.0/). Any further distribution of this work must maintain attribution to the author(s) and the title of the work, journal citation and DOI.

**Contents**

<b>1. Introduction</b>	<b>2</b>
<b>2. Results and discussion</b>	<b>3</b>
<b>3. Conclusions</b>	<b>8</b>
<b>Acknowledgments</b>	<b>9</b>
<b>References</b>	<b>9</b>

**1. Introduction**

The future development of transparent and flexible electronics depends on the ability to engineer conductive and semiconducting materials which are mechanically flexible and optically transparent [1, 2]. Graphene—a single layer of carbon atoms with a honeycomb structure—meets most of the requirements for flexible electronics [3]. This is the most flexible transparent material [4–6] which can be doped with  $\text{FeCl}_3$  to become also the best known transparent electrical conductor [7]. However, in its pristine form, graphene does not have a band gap in the energy dispersion [8], and this prevents the full exploitation of the potential of this material in transistor applications where a large on/off ratio of the current is required. A variety of techniques are currently under investigation to engineer a band-gap in graphene materials, such as an electric field induced band-gap in few-layer graphene [9, 10], quantum confinement—e.g. nanoribbons [11] and quantum dot structures [12]—and chemical functionalization [13–20]. The latter is currently attracting a growing interest since it is typically simple to implement and to scale up to wafer size for industrial production.

The opening of a band-gap via chemical functionalization typically involves a change of the  $sp^2$  hybridization of the electronic orbitals characteristic of pristine graphene to a tetragonal  $sp^3$  orbital. Depending on the chemical specie employed in the functionalization process, it is possible to turn graphene into a wide or narrow gap semiconductor. For example, fluorinated graphene has a band-gap of  $\geq 4$  eV [21–23] and this functionalization is thermodynamically stable at temperatures as high as  $400^\circ\text{C}$  [18]. In contrast to other methods, chemical functionalization is expected to open a band-gap which is robust against disorder as long as the mean free path of the electrons is large compared to the average distance between adatoms [24]. In this case, the value of the band-gap is also expected to depend on the degree of functionalization—i.e. coverage of adatoms [24]. Though this prediction considerably widens the potential of chemically functionalized graphene, it has not yet been demonstrated experimentally due to the difficulty to tune continuously the coverage of adatoms in the functionalization process.

In this paper we demonstrate experimentally that the energy gap  $\epsilon_1$  between the localized states and the mobility edge of the valence band in chemically functionalized graphene, can be tuned in partially fluorinated graphene (PFG) by changing the coverage of fluorine adatoms simply via electron-beam irradiation. From a detailed study of the temperature dependence of the resistance (from 4.2 K up to room temperature), we find that the electrical conduction in PFG takes place via thermally activated carriers over the energy gap  $\epsilon_1$ . We show that in flakes exfoliated from  $\text{CF}_{0.28}$  this energy gap decreases monotonically upon electron irradiation. At the same time we find that PFG displays an insulator to metal transition upon reducing the fluorine coverage. In particular, for low irradiation doses ( $< 0.1 \text{ C cm}^{-2}$ ) the electrical

conduction in this material is described well by the lightly doped semiconductor model [32] characteristic of standard semiconductors such as germanium and silicon. On the other hand, for high irradiation doses ( $>0.2 \text{ C cm}^{-2}$ ), electrical conduction takes place via Mott variable range hopping (MVRH).

## 2. Results and discussion

The chemical functionalization of graphene with fluorine adatoms is obtained by exposing natural graphite to  $\text{F}_2$  atmosphere at  $450^\circ\text{C}$ . Upon functionalization, the planar layer structure of each graphene sheet composing the bulk graphite is transformed into a three-dimensional structure with covalently bonded fluorine atoms above and below the plane of the sheet. The percentage of the fluorine coverage is determined via gravimetry (mass uptake) and further confirmed by solid state NMR measurements [26–28]. Subsequently, flakes of few-layer PFG were isolated by mechanical cleavage of bulk fluorinated graphite ( $\text{CF}_{0.28}$ ) onto a p-doped Si substrate—which acts as a back gate—covered by a 285 nm thick layer of  $\text{SiO}_2$ . PFG flakes are identified via their low optical contrast, typically 2–4% for few layers with white light. Electrical contacts are fabricated using standard electron beam lithography and thermal evaporation of Cr/Au contacts (5/70 nm) followed by a lift-off process in acetone. The zero-bias resistance of the devices was measured in a constant voltage configuration with a lock-in amplifier, where the excitation voltage was varied to ensure that the energy range where electrical transport takes place is smaller than the energy range associated to the temperature of the electrons ( $eV_b < k_B T$ ). This prevents heating of the electrons and the occurrence of non-equilibrium effects. In these studies we employ two terminal electrical measurements in transistor devices with a negligible contact resistance at the metal/fluorinated graphene interface as compared to the sample resistance (see supporting information, available from [stacks.iop.org/NJP/15/033024/mmedia](http://stacks.iop.org/NJP/15/033024/mmedia)).

We change *in situ* the level of fluorine coverage by irradiating the samples with an incident electron beam of 10 keV energy and a current of 0.13 nA. Under these conditions, secondary electrons generated from the primary beam and from the backscattered electrons break the C–F bonds with an efficiency of  $\sim 5 \times 10^{-5}$ , whereas the electrical properties of pristine multilayer samples are not significantly affected [29]. To prevent electrical discharges from damaging the device during the irradiation process, the contacts and the back gate are kept connected to ground. In total we have studied more than five different samples which behaved similarly under the same electron-irradiation conditions.

Figure 1(a) shows a plot of a typical zero-bias square resistance ( $R_{\text{sq}}$ ) measured at room temperature after different steps of electron irradiation which correspond to different fluorine coverage. The starting material is the electrically insulating PFG with 28% coverage ( $\text{CF}_{0.28}$ ) and  $R_{\text{sq}} \approx 1 \text{ T}\Omega$ . Upon reducing the fluorine coverage we find that  $R_{\text{sq}}$  decreases monotonically down to  $\approx 10 \text{ K}\Omega$  after exposure to  $1 \text{ C cm}^{-2}$ . Such low values of  $R_{\text{sq}}$  are typical of pristine graphene samples and suggest that electron irradiation has reduced PFG to the pristine form. A measurement of the back-gate dependence of  $R_{\text{sq}}$  reveals that PFGs are hole-doped (see inset in figure 1(a)).

At the same time, the temperature dependence of  $R_{\text{sq}}$  measured after different dose exposures shows that PFG undergoes an insulator to metal transition driven by the decrease of fluorine coverage (see figure 1(b)). In particular, for  $\text{CF}_{0.28}$  the  $R_{\text{sq}}$  diverges when lowering the temperature, as expected for insulating materials. After irradiating to  $1 \text{ C cm}^{-2}$  and after

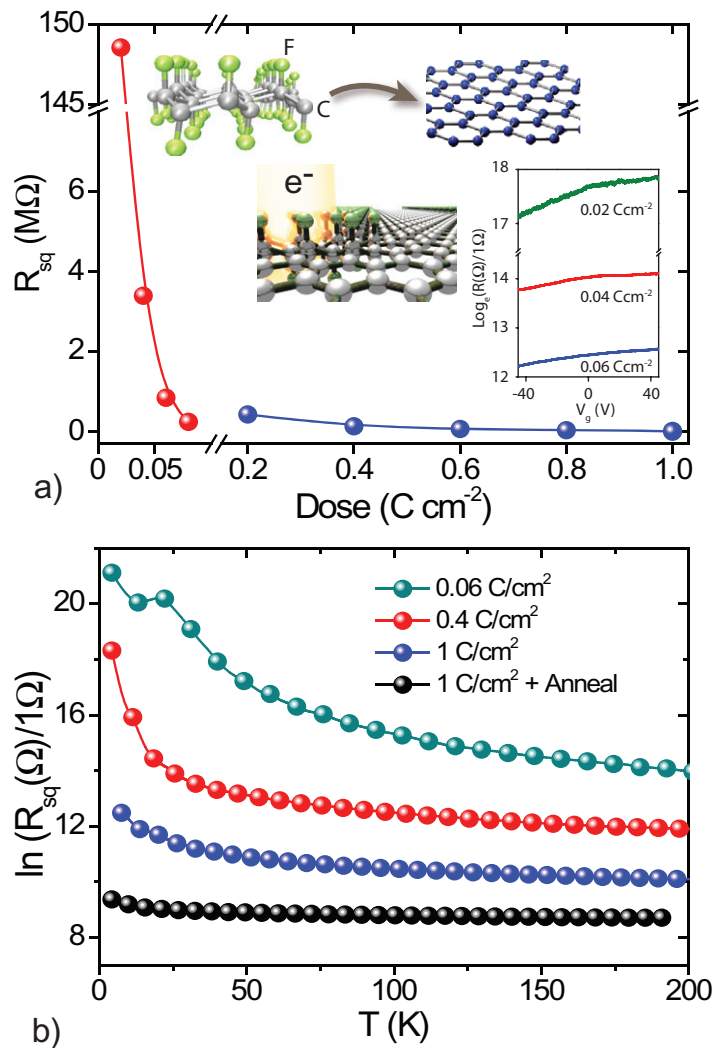


**Figure 1.** (a) Plot of the zero-bias square resistance ( $R_{sq}$ ) measured at room temperature after different steps of electron beam irradiation for a representative sample. The cartoon in the inset shows a sketch of the electron-irradiation induced defluorination process. The graph in the inset shows a plot of the gate dependence of  $R_{sq}$  after irradiation with different doses. (b) Plot of the temperature dependence of the  $\ln(R_{sq})$  after subsequent electron irradiation steps. A transition from an insulating state in  $CF_{0.28}$  to a metallic state is observed after complete defluorination by exposure to a dose of  $1\ C\ cm^{-2}$ .

conducting a mild annealing to remove contaminants from the surface [29], the samples exhibit a very weakly temperature dependent  $R_{sq}$  which is typical of pristine graphene [30].

We first present the experimental characterization of PFG exposed to low electron beam irradiation corresponding to doses ranging from 0 up to  $0.1\ C\ cm^{-2}$  in steps of  $0.02\ C\ cm^{-2}$  (see figure 1(a)). To understand the nature of the electrical conduction in these materials we consider a semilog plot of the inverse temperature dependence of  $R_{sq}$  for a representative sample (see figures 2(a)–(b) and supporting information, available from [stacks.iop.org/NJP/15/033024/mmedia](http://stacks.iop.org/NJP/15/033024/mmedia)). In all cases we find that  $\ln(R_{sq})$  has a similar functional

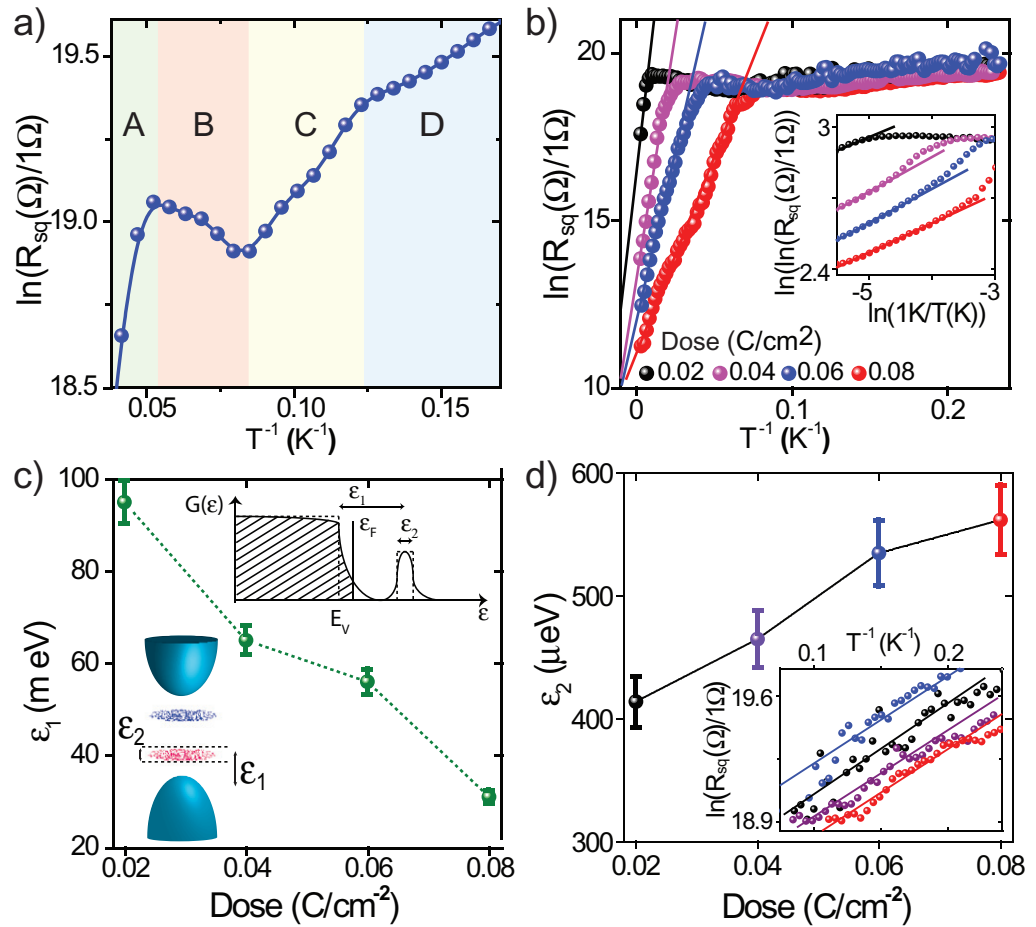


**Figure 2.** (a) Semilog plot of the high resistive region of the inverse temperature dependence of  $R_{sq}$  for a  $CF_{0.28}$  sample in the temperature range  $<30$  K after exposure to  $0.06 \text{ C cm}^{-2}$ . The four regions (A, B, C and D) with distinct slopes of  $\ln(R_{sq})$  versus  $T^{-1}$  characteristic of lightly doped semiconductors are highlighted on the graph. (b) Full-scale semilog plot of the inverse temperature dependence of  $R_{sq}$  for samples irradiated to different electron doses and measured up to room temperature. The continuous lines are linear fits to the exponential dependence of the resistance in region A due to thermally activated carriers across the energy gap  $\epsilon_1$ . The plot in the inset highlights the exponential dependence of the resistance in A by presenting a double-log scale plot. (c) Shows a plot of the energy gap  $\epsilon_1$  between the impurity states and the valence band edge and  $\epsilon_2$  the impurity band width. The top inset shows a sketch of the density of states versus energy for PFG, whereas the bottom inset shows a sketch of the energy dispersion in PFG. (d) Plot of the hopping conduction activation energy extracted from the linear fit of the semilog inverse temperature dependence of  $R$  for different doses of electron irradiation shown in the inset.

dependence on  $T^{-1}$  characterized by four regions with distinct slopes (regions A, B, C and D highlighted in figure 2(a) which focuses on the low temperature range  $T < 30$  K behavior extracted from the plots in figure 2(b)). We note that this particular temperature dependence is

identical to the well established temperature dependence of lightly doped semiconductors [32]. This similarity suggests that PFG is a semiconductor with impurity states in the band gap. Previous studies in standard semiconductors [32] have established that region A corresponds to intrinsic electrical conduction due to thermally activated carriers across the energy gap  $\epsilon_1$  between the localized states and the mobility edge of the valence or conduction band depending on the position of the chemical potential in the system. At sufficiently low temperatures the intrinsic charge carriers become less than the concentration contributed by the impurities. In these regions, i.e. B to D, the conduction is entirely determined by the nature and concentration of impurities. In what follows we adopt the lightly doped semiconductor model to explain the evolution of the energy dispersion in fluorinated graphene as a function of F-coverage.

The intrinsic carrier concentrations of electrons and holes in region A gives an exponential dependence of the resistance on temperature:  $R(T) = R_0 e^{\frac{\epsilon_1}{2k_B T}}$  where  $\epsilon_1$  is the energy gap between the impurity states and the valence band edge. Due to the impurity and/or defect induced states,  $\epsilon_1$  in these PFG is smaller than the true energy gap corresponding to the difference between the top and bottom of the valence and valence bands (see inset in figure 2(c)). The value of  $\epsilon_1$  and its dependence on the electron irradiation are readily determined from a linear fit to the plot of  $\ln(R_{sq})$  versus  $T^{-1}$  for region A after different low dose irradiation (up to  $0.08 \text{ C cm}^{-2}$ ), see figure 2(c). We find that  $\epsilon_1$  decreases monotonously from  $\approx 90 \text{ meV}$  (after irradiation to  $0.02 \text{ C cm}^{-2}$ ) to  $\approx 30 \text{ meV}$  (after irradiation to  $0.08 \text{ C cm}^{-2}$ ).

In lightly doped semiconductors [31, 32], upon lowering the temperature the systems enter the so-called saturation range. Here all impurities are ionized and the carrier concentration in the band is nearly temperature independent. At the same time, upon lowering the temperature we observe a reduction of  $R_{sq}$  due to an increase of the mobility. This is likely to be the consequence of a reduction of the electron scattering rates due to ion impurity scattering, whereas electron phonon scattering is not relevant since PFG has low values of charge carrier mobilities [31, 32]. This is region B for PFG. The subsequent range is known as the freezing-out range (region C), where the extrinsic charge carriers are recaptured by the defects and/or impurities. In this region the temperature dependence of the sample resistance is commonly described by  $R_T = R_3 e^{\frac{\epsilon_2}{2k_B T}}$  with an activation energy  $\epsilon_2$  which is much smaller than  $\epsilon_1$  [32]. In particular, we find that  $\epsilon_2$  is enhanced from  $\approx 0.4 \text{ meV}$  after irradiation to  $0.02 \text{ C cm}^{-2}$  to a value of  $\epsilon_2 \approx 0.55 \text{ meV}$  after exposure to a dose of  $0.08 \text{ C cm}^{-2}$ , see figure 2(d). The observed increase of  $\epsilon_2$  upon electron irradiation is possibly due to an increase of random Coulomb potential associated with the dangling bonds created by the irradiation-assisted defluorination process. Finally, at the lowest temperatures in region D the main contribution to the electrical conductivity comes from electrons hopping directly between localized states at sub-gap energies.

We now turn our attention to the higher dose regime, which corresponds to a lower coverage of fluorine adatoms. Figure 3(a) shows a semilog plot of the temperature dependence of the square resistance after various electron beam irradiations from a dose of  $0.2$  up to  $1 \text{ C cm}^{-2}$ . In all cases we find that at high enough temperatures the conduction in these samples takes place via hopping through localized states with  $R(T) \propto e^{\frac{\epsilon_a}{2k_B T}}$  and  $\epsilon_a$  the hopping activation energy. This temperature range corresponds to region C and the values of  $\epsilon_a$  extracted from the fits are plotted in figure 3(b). It is apparent that  $\epsilon_a$  shows a monotonic decrease with increasing dose.

Upon lowering the temperature the  $\ln(R_{sq})$  is nonlinear in  $T^{-1}$ , indicating that another mechanism of conduction is at play in this D region (see figure 3(a)). To identify the specific hopping mechanism of conduction dominating in D, we consider the generic expression  $R(T) = R_0 e^{(T_0/T)^p}$  where  $p$  is a parameter that depends on the dimensionality of the system as well as the

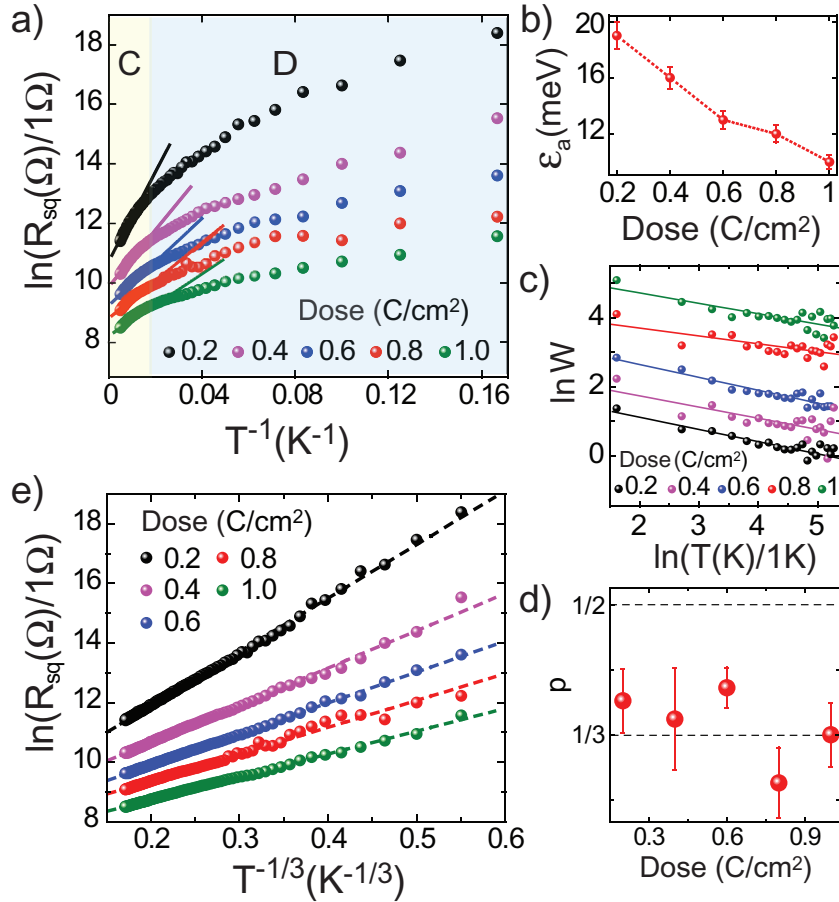


**Figure 3.** (a) Semilog plot of the inverse temperature dependence of  $R_{sq}$  after various high dose irradiation steps as indicated in the graph. The continuous lines are a fit to thermally activated transport. (b) Plot of the activation energy of the hopping conduction via localized states as a function of electron dose irradiation extracted from the linear fits in (a). (c) Logarithmic scale plot of  $W = -\ln(R(T))/\ln(T)$  versus temperature, the continuous lines are fit to  $W = p(T_0/T)^p$  and (d) shows the best fit values for  $p$  for each given electron dose irradiation. (e) Shows a semilog plot of  $R_{sq}$  as a function of  $T^{-1/3}$ , the dashed lines are fit to the MVRH.

conduction mechanism and  $T_0$  is the characteristic temperature of the system which correlates to the degree of localization. For a two-dimensional system—such as fluorinated graphene— $p$  is equal to 1 for thermally activated transport,  $1/2$  for Efros–Shklovskii variable range hopping and  $1/3$  for MVRH [25]. The exponent  $p$  can be determined from a linear fit to the logarithm of the reduced activation energy versus  $\ln T(K)/1K$ , where the reduced activation energy is defined by the relation  $W = -\ln R(T)/\ln T = p(T_0/T)^p$ , see figures 3(c) and (d) [33]. We find that for all the studied doses the best fit gives  $p = 1/3$ , demonstrating that the electrical conduction takes place by MVRH. From a fit of  $R(T)$  to MVRH conduction mechanism (see figure 3(e)) we can extract the values of  $T_0$  for each different electron dose irradiation. This hopping parameter is shown in figure 4(a) and it is found to decrease with increasing the electron dose therefore suggesting an increased density of sub-gap states and of localization radius.



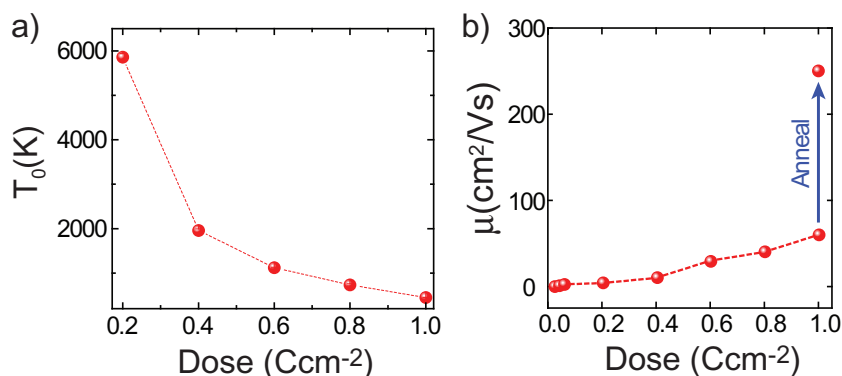


**Figure 4.** Graphs in (a) and (b) show the characteristic temperature  $T_0$  of the MVRH mechanism and the field effect mobility as a function of electron beam dose irradiation.

A two-dimensional tight binding theoretical model predicts that an energy gap whose value depends on the coverage of adatoms is expected in the limit that the mean free path of charge carriers is longer than the average distance between adatoms [24]. In this case, assuming an asymmetry between the graphene sublattices, the Bragg scattering of electron waves by the adatoms opens a uniform energy gap which is immune to the positional disorder of the adatoms. Although the structure of PFG is not two-dimensional and an extension of the theoretical model by Abanin *et al* [24] to capture the tetragonal  $sp^3$  bonds is needed, we note that in our experiments the mean free path in this low-dose regime is always longer than the distance between fluorine adatoms. The charge carrier mobilities in PFG are typically of the order of  $10 \text{ cm}^2 \text{ V s}^{-1}$  (see figure 4(b)). The Fermi velocity in PFG is  $v_F = \sqrt{\frac{2n\pi\hbar^2}{em^*}}$  with  $n$  charge density,  $e$  the charge of the electron and  $m^*$  the effective mass in fluorinated graphene [22]. Therefore the typical mean free path for charge carriers in our devices is  $l = \frac{\hbar\mu}{e} \sqrt{\frac{2n\pi}{e}} \approx 1.5 \text{ nm}$ . Thus we can expect that also in our PFG materials Bragg scattering of electron waves plays a primary role in opening a uniform energy gap down to a F-coverage of 0.72% which is the concentration at which the average distance between adatoms becomes equal to the charge carriers mean free path. Since electron-irradiation is a simple method to control the fluorine functionalization in PFG, our experiments show that PFG might be an easier system where to study the interplay between Bragg scattering of electron waves and adatoms in opening a uniform band gap. However, an extension of the previously developed two-dimensional model [24] is needed.

### 3. Conclusions

In conclusion we show that the energy gap  $\epsilon_1$  between the localized states and the mobility edge of the valence band in PFG can be tuned by changing the coverage of fluorine adatoms simply via electron-beam irradiation. We show that in  $\text{CF}_{0.28}$  this energy gap decreases monotonically upon electron irradiation up to a dose of  $0.08 \text{ C cm}^{-2}$ . At the same time, these PFG materials display an insulator to metal transition when decreasing the coverage of fluorine adatoms. In particular, for low doses of electron beam irradiation, PFG is a lightly doped semiconductor with an intrinsic energy gap whose value depends on the fluorine coverage. For higher doses,

the transport is governed by MVRH. These experimental findings highlight that electron beam irradiation of fluorinated graphene is a novel way to engineer energy gaps in graphene materials.

## Acknowledgments

SR and MFC acknowledge financial support from EPSRC (grant numbers EP/G036101/1, EP/J000396/1, EP/K017160/1 and EP/K010050/1). SR acknowledges financial support from the Royal Society Research grant number 2010/R2 (grant number SH-05052).

## References

- [1] Rogers J A, Someya T and Huang Y 2010 *Science* **327** 1603
- [2] Nomura K, Ohta H, Takagi A, Kamiya T, Hirano M and Hosono H 2004 *Nature* **432** 488
- [3] Geim A K 2009 *Science* **324** 1530
- [4] Kim K S, Zhao Y, Jang H, Lee S Y, Kim J M, Kim K S, Ahn J H, Kim P, Choi J Y and Hong B H 2009 *Nature* **457** 706
- [5] Nair R R, Blake P, Grigorenko A N, Novoselov K S, Booth T J, Stauber T, Peres N M R and Geim A K 2008 *Science* **320** 1308
- [6] Bae S *et al* 2010 *Nature Nanotechnol.* **5** 574
- [7] Khrapach I, Withers F, Bointon T H, Polyushkin D K, Barnes W L, Russo S and Craciun M F 2012 *Adv. Mater.* **24** 2844
- [8] Wallace P R 1947 *Phys. Rev.* **71** 622
- [9] Craciun M F, Russo S, Yamamoto M and Tarucha S 2011 *Nano Today* **6** 42
- [10] Zhang Y, Tang T-T, Girit C, Hao Z, Martin M C, Zettl A, Crommie M F, Shen Y R and Wang F 2009 *Nature* **459** 820
- [11] Son Y-W, Cohen M L and Louie S G 2006 *Phys. Rev. Lett.* **97** 216803
- [12] Ponomarenko L A, Schedin F, Katsnelson M I, Yang R, Hill E W, Novoselov K S and Geim A K 2008 *Science* **320** 356
- [13] Withers F, Dubois M and Savchenko A K 2010 *Phys. Rev. B* **82** 073403
- [14] Withers F, Russo S, Dubois M and Craciun M F 2011 *Nanoscale Res. Lett.* **6** 526
- [15] Ryu S, Han M Y, Maultzsch J, Heinz T F, Kim P, Steigerwald M L and Brus L E 2008 *Nano Lett.* **8** 4597
- [16] Bon S B, Valentini L, Verdejo R, Garcia Fierro J L, Peponi L, Lopez-Manchado M A and Kenny J K 2009 *Chem. Mater.* **21** 3433
- [17] Elias D C *et al* 2009 *Science* **323** 610
- [18] Nair R R *et al* 2010 *Small* **6** 2877
- [19] Zhang H, Bekyarova E, Huang J-W, Zhao Z, Bao W, Wang F, Haddon R and Lau C N 2011 *Nano Lett.* **11** 4047
- [20] Chuang C, Puddy R K, Lin H-D, Lo S-T, Chen T M, Smith C G and Liang C-T 2012 *Solid State Commun.* **152** 905
- [21] Boukhalov D W and Katsnelson M I 2009 *J. Phys.: Condens. Matter* **21** 344205
- [22] Leenaerts O, Peelaers H, Hernandez-Nieves A, Partoens B and Peeters F 2010 *Phys. Rev. B* **82** 1
- [23] Sahin H, Topsakal M and Ciraci S 2011 *Phys. Rev. B* **83** 115432
- [24] Abanin D A, Shtyov A V and Levitov L S 2010 *Phys. Rev. Lett.* **105** 86802
- [25] Shklovskii B I and Efros A L 1984 *Electronic Properties of Lightly Doped Semiconductors (Springer Series in Solid State Sciences vol 45)* (Berlin: Springer)
- [26] Chamssedine F, Dubois M, Guerin K, Giraudet J, Masin F, Ivanov D A, Vidal L, Yazami R and Hamwi A 2006 *Chem. Mater.* **19** 161
- [27] Dubois M, Giraudet J, Guerin K, Hamwi A, Fawal Z, Pirotte P and Masin F 2006 *J. Phys. Chem. B* **110** 11800

- [28] Zhang W, Dubois M, Guerin K, Bonnet P, Kharbache H, Masin F, Kharitonov A P and Hamwi A 2010 *Phys. Chem. Chem. Phys.* **12** 1388
- [29] Withers F, Bointon T H, Dubois M, Russo S and Craciun M F 2011 *Nano Lett.* **11** 3912
- [30] Tan Y-W, Zhang Y, Stormer H L and Kim P 2007 *Eur. Phys. J. Spec. Top.* **148** 15
- [31] Ando T, Fowler A B and Stern F 1982 *Rev. Mod. Phys.* **54** 437
- [32] Efros A L and Shklovskii B I 1985 *Electron–Electron Interactions in Disordered Systems* (Amsterdam: North-Holland)
- [33] Zhang Y, Dai O, Levy M and Sarachik M P 1990 *Phys. Rev. Lett.* **64** 2687